Mapping the human brain at rest with diffuse optical tomography

Brian R. White, Abraham Z. Snyder, Alexander L. Cohen, Steven E. Petersen, Marcus E. Raichle, Bradley L. Schlaggar, Joseph P. Culver

Abstract— **Diffuse optical tomography (DOT) is a portable functional neuroimaging technique that is able to simultaneously measure both oxy- and deoxyhemoglobin responses to brain activity. Herein, we demonstrate a technique for mapping functional connections in the brain by measuring the spatial distribution of temporal correlations in resting brain activity. Simultaneous DOT imaging over the motor and visual cortices yielded robust correlation maps reproducing the expected functional neural architecture. These functional connectivity methods will have utility in certain populations, such as those who are unconscious or very young, who have difficulty performing the behaviors required in traditional task-based functional neuroimaging paradigms.**

I. INTRODUCTION

THE majority of functional neuroimaging studies have focused on applying external stimuli and measuring responses in hemodynamic imaging contrasts. Within this perspective, spontaneous fluctuations in the brain's hemodynamics have been considered "noise" or at best "nuisance" signals. However, recent work in functional magnetic resonance imaging (fMRI) has found that temporal correlations in spontaneous activity between different brain regions represent functional connections[1]. Thus, the functional organization of the human brain can be mapped through analysis of these resting-state networks (RSNs). Herein, we examine a method for mapping resting state functional connectivity using non-invasive diffuse optical tomography (DOT) of the human brain. The combination of resting-state methodology with DOT, which is portable and enables measurement of comprehensive hemodynamic contrasts, could allow a powerful tool for bedside neurological assessment of infants and critically ill patients.

We have previously developed a high performance DOT system capable of detailing functional activations[2]. In this work, we use the system to evaluate a novel spatial mapping of functional connectivity (fc-DOT) [3]. To specifically address our goal of fc-DOT mapping, we extended the field-of-view of our DOT system to provide simultaneous high-density imaging of distributed cortical regions covering both the visual and motor cortices. These unique spatial capabilities are complemented by linear regression methods that remove global superficial signals and correlation analyses to map spontaneous brain activity patterns.

We judge the success of fc-DOT by our ability to obtain spatial correlations maps based on local physiology that match the fc-MRI literature and our own subject-matched fc-MRI experiments. Functional connectivity was first demonstrated by BOLD-fMRI detecting low-frequency variations in the motor cortex in the resting state[4]. Previous fc-MRI studies have also demonstrated that the motor and visual cortices constitute largely independent functional networks, each exhibiting high levels of inter-hemispheric correlation[5, 6]. We, thus, expect correlation mapping using a seed region within a somatomotor task response region to specifically reveal the somatomotor network. Similarly, a seed within a visual response area should generate a resting state correlation map specific to the visual system.

II. METHODS

A. Protocol.

Healthy adult subjects were recruited (4 female and 1 male, ages 24-27). Stimulus studies were performed to locate the motor and visual cortices. The visual cortex was stimulated using pseudorandom blocks of right and left lower visual quadrant reversing checkerboard grids (10 Hz reversal on 50% gray background, 10 s on and 20 s off). The somatomotor cortex was stimulated with pseudorandom blocks of right and left finger tapping (self-paced at about 3 Hz, 10 s on and 20 s off). For resting-state analysis, a 50% gray screen with a crosshair was viewed (in 5 min blocks for 10 or 15 min total).

B. DOT Imaging.

DOT imaging arrays were placed over the visual (24 sources, 28 detectors, Fig. 1a) and somatomotor (24 sources, 18 detectors, Fig 1b) cortices and held in place with hook-

B. R. White, is with the *Department of Physics, and Department or Radiology, Washington University, St. Louis, MO*

A.Z. Snyder, is with the *Department of Neurology, and Department or Radiology, Washington University, St. Louis, MO*

A.L. Cohen, is with the *Department of Neurology, Washington University, St. Louis, MO*

S.E. Petersen, is with the *Department of Neurology, and Department or Radiology, Washington University, St. Louis, MO*

M.E. Raichle, is with the *Department of Neurology, and Department or Radiology, Washington University, St. Louis, MO*

B.L. Schlaggar, is with the *Department of Neurology, and Department or Radiology, Washington University, St. Louis, MO*

J.P. Culver, is with the *Department of Physics, and Department or Radiology, Washington University, St. Louis, MO:* phone: 314-747-1341; fax: 314-747-5191; e-mail: culverj@wustl.edu.

and-loop strapping[2]. The position of the pads relative to the nasion and inion was measured to establish repeatable positioning. Data were converted to log-ratio and high-pass filtered (0.02 Hz for stimulus data, 0.009 Hz for resting-state data) to remove long-term drift. An average of all 1st-nearest-neighbor measurements was regressed from all measurements within each pad. After a low-pass filter (0.5 Hz) removed residual pulse signals, the time traces were used for image reconstruction. Prior to inversion, channels with high standard deviation (change in intensity >7.5%) within a given run were removed from the reconstruction to reduce image noise due to such artifacts as optode motion. A two-layer head model was used with finite-element software (NIRFAST)[7] to generate a light-sensitivity matrix of the DOT arrays. The mesh contained 22,731 nodes, and after light modeling the sensitivity matrix was interpolated to a 2 mm square voxel-grid. This sensitivity matrix was inverted once per subject per run (in order to account for the specific channels included), a process which takes 33 s. The inverted sensitivity matrix converts time series measurement data into a series of three-dimensional images of differential absorption for each wavelength. Changes in the concentrations of HbO_2 and HbR were then obtained using their extinction coefficients. For further reconstruction details, see our earlier publication[2]. A cortical shell (1 cm thickness) was selected and all images shown are projections of this shell (Visual: posterior coronal view, Motor: superior horizontal view, Fig. 1c-d).

C. fc-DOT Analysis.

Functional response images were obtained by block-averaging each subject's trials and temporally averaging (5 s)
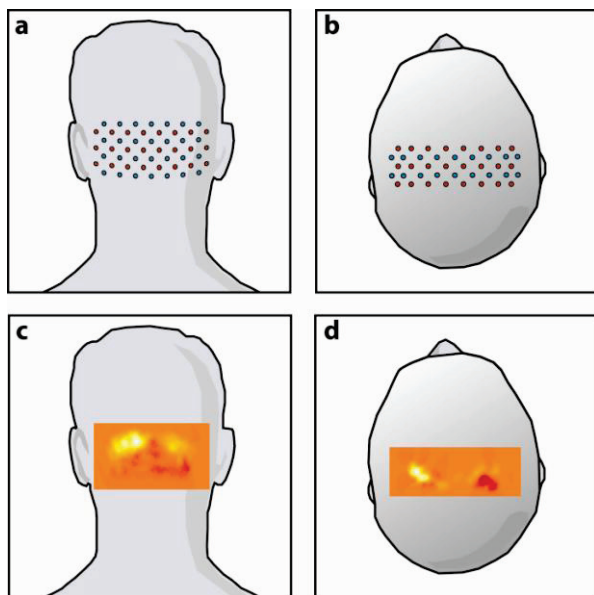
Fig. 1. (a) Our DOT imaging system with functional responses. **(a)** Schematic of the visual cortex imaging pad (24 sources, red, and 28 detectors, blue). **(b)** Schematic of the motor cortex imaging pad (24 sources, red, and 18 detectors, blue). **(c)** A left visual cortex response (ΔHbO_2), posterior coronal projection of a cortical shell. **(d)** A motor cortex response (ΔHbO_2), superior axial projection of a cortical shell

around the peak hemodynamic response. For each of the four regions of interest (left/right visual and left/right motor cortices) and for each subject, a 1 cm^3 volume was chosen as a seed region for correlation analysis. Resting-state images were low-pass filtered (0.08 Hz). The resting state time traces from within each seed volume were averaged to create a seed signal, and correlation coefficients were calculated between the seed signal and every other voxel in the field-of-view of both imaging pads.

III. RESULTS

With our extended DOT system, we simultaneously imaged with DOT arrays placed over the visual and motor cortices (Fig. 1a-b). Task paradigms were performed to locate the motor and visual cortices within each subject, yielding functional responses with high contrast-to-noise (Fig. 1c-d). Examples of the resting state time courses are shown in figure 2. Evaluation of the fcDOT maps are shown figure 3. For comparison to fMRI we evaluated fc-MRI maps from the same subject scanned with fcDOT. Note the high inter-hemispheric correlations and low correlations between the motor and visual networks for both fc-DOT and fc-MRI.
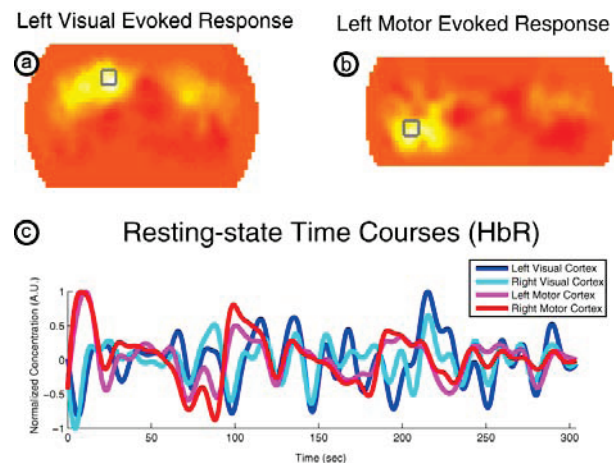
Fig.2. Correlation analysis between both visual and motor cortices from resting state data measured for 5 min. **(a)** Right and left visual cortex seed regions were determined using an activation paradigm. Shown is the left visual response with right and left seeds shown with gray boxes. **(b)** Right and left motor cortex seed regions were determined using an activation paradigm. Shown is the left motor response with right and left seeds shown with gray boxes. **(c)** Normalized time courses from resting state measurements. The two visual cortices are correlated (0.71), the two motor cortices are correlated (coefficient coefficient 0.89), but motor and visual are uncorrelated with each other (coefficients -0.19±0.05).

IV. CONCLUSION

These results demonstrate the successful application of functional connectivity methods to DOT of adult human subjects. New high-density DOT systems may offer the resolution, signal-to-noise, and system simplicity that allow optical imaging to successfully translate to widespread use. Our results validate DOT functional connectivity methods (fc-DOT) within a model system established by fMRI. Such an approach increases our confidence in the fidelity of fc-

DOT, providing a strong foundation for moving RSN analysis beyond the studies that fMRI is capable of performing. We look forward to extending the fc-DOT methods presented here to study questions of interest in contemporary neuroscience in the areas of brain disease, development, and physiology.
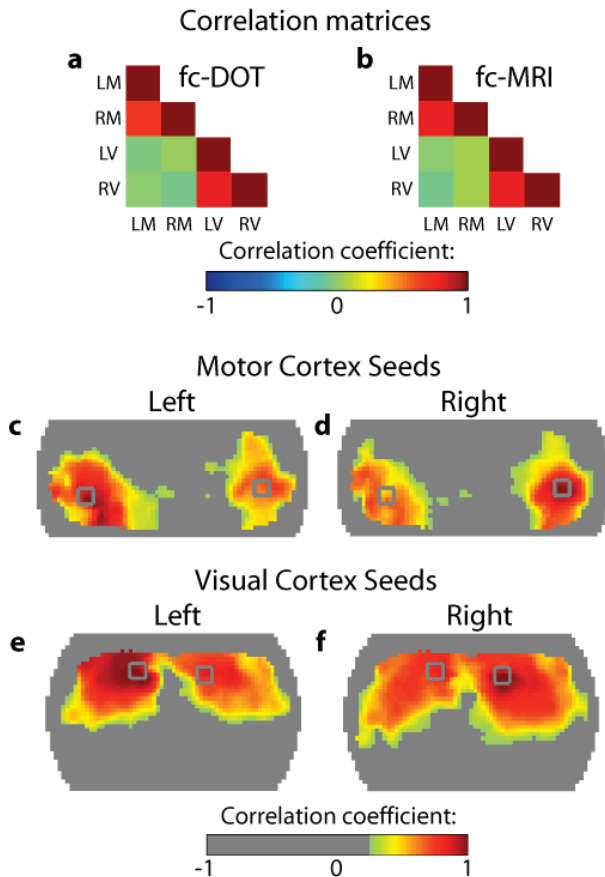
Fig. 3. Analysis of fcDOT methods. Correlation coefficients were evaluated using four seed regions at the following positions - LM: left motor cortex, RM: right motor cortex, LV: left visual cortex, RV: right visual cortex. **(a)** Cross-correlation matrix for all four seeds from fc-DOT imaging. Note the high inter-hemispheric correlations and low correlations between the motor and visual networks. **(b)** Cross-correlation matrix for four similar seed regions from fc-MRI performed in the same subject. Note the similarity to the fc-DOT correlation matrix. **(c-d)** fc-DOT correlation map using the left and right motor cortex seed. **(e-f)** fc-DOT using the left and right visual cortex seeds. The color scale has a threshold at r=0.25.

REFERENCES

[1]   M. D. Fox and M. E. Raichle, "Spontaneous fluctuations in brain activity observed with functional magnetic resonance imaging," *Nature Reviews Neuroscience*, vol. 8, pp. 700-711, 2007.

[2]   B. W. Zeff, B. R. White, H. Dehghani, B. L. Schlaggar, and J. P. Culver, "Retinotopic mapping of adult human visual cortex with high-density diffuse optical tomography," *PNAS*, vol. 104, pp. 12169-12174, 2007.

[3]   B. R. White, A. Z. Snyder, A. L. Cohen, S. E. Petersen, M. E. Raichle, B. L. Schlaggar, and J. P. Culver, "Resting-state functional connectivity in the human brain revealed with diffuse optical tomography," *Neuroimage*, vol 47, pp 148-156, 2009.

[4]   B. Biswal, F. Z. Yetkin, V. M. Haughton, and J. S. Hyde, "Functional Connectivity in the Motor Cortex of Resting Human Brain Using Echo-Planar MRI," *Magnetic Resonance in Medicine*, vol. 34, pp. 537-541, 1995.

[5]   M. De Luca, C. F. Beckmann, N. De Stefano, P. M. Matthews, and S. M. Smith, "fMRI resting state networks define distinct modes of long-distance interactions in the human brain," *NeuroImage*, vol. 29, pp. 1359-1367, 2006.

[6]   J. S. Damoiseaux, S. A. R. B. Rombouts, F. Barkhof, P. Scheltens, C. J. Stam, S. M. Smith, and C. F. Beckmann, "Consistent resting-state networks across healthy subjects," *Proceedings of the National Academy of Sciences of the United States of America*, vol. 103, pp. 13848-13853, 2006.

[7]   H. Dehghani, B. W. Pogue, S. P. Poplack, and K. D. Paulsen, "Multiwavelength three-dimensional near-infrared tomography of the breast: initial simulation, phantom, and clinical results," Applied Optics, vol. 42, pp. 135-145, 2003.